Published in final edited form as:
J Immunol. 2014 January 1; 192(1): 41–51. doi:10.4049/jimmunol.1301277.

Munc18-2 and Syntaxin 3 control distinct essential steps in mast cell degranulation[1]

Cristiana Brochetta[#*,†,3], **Ryo Suzuki**[#‡], **Francesca Vita**[§], **Maria Rosa Soranzo**[§], **Julien Claver**[*,†], **Lydia Celia Madjene**[*,†], **Tarik Attout**[*,†], **Joana Vitte**[*,†,4], **Nadine Varin-Blank**[¶,‖], **Giuliano Zabucchi**[§], **Juan Rivera**[‡], and **Ulrich Blank**[*,†,5]

[*]Inserm UMRS-699, 75018 Paris, France

[†]Université Paris Diderot, Sorbonne Paris Cite, Laboratoire d'excellence INFLAMEX, 75018 Paris, France

[‡]Laboratory of Molecular Immunogenetics, National Institute of Arthritis and Musculoskeletal and Skin Diseases, National Institutes of Health, Bethesda, MD, 20892

[§]Department of Life Sciences Department of Physiology and Pathology, University of Trieste, Italy

[¶]Inserm U978, 93000 Bobigny, France

[f]Université Paris 13, Sorbonne Paris Cité, "Adaptateurs de Signalisation en Hématologie,"

[‖]Laboratoire d'excellence "Inflamex," Unité de Formation et de Recherche Santé-Médecine-Biologie Humaine, 93000 Bobigny, France

[#] These authors contributed equally to this work.

Abstract

Mast cell degranulation requires N-ethylmaleimide-sensitive factor attachment protein receptors (SNAREs)[6] and mammalian unc18 (Munc18) fusion accessory proteins for membrane fusion. However, it is still unknown how their interaction supports fusion. Here we found that siRNA-mediated silencing of the isoform Munc18-2 in mast cells inhibits cytoplasmic secretory granule (SG) release but not CCL2 chemokine secretion. Silencing of its SNARE binding partner Syntaxin 3 (STX3) also markedly inhibited degranulation, while combined knock-down produced an additive inhibitory effect. Strikingly, while Munc18-2 silencing impaired SG translocation, silencing of STX3 inhibited fusion demonstrating unique roles of each protein. Immunogold studies showed that both Munc18-2 and STX3 are located on the granule surface, but also within the granule matrix and in small nocodazole-sensitive clusters of the cytoskeletal meshwork surrounding SG. After stimulation clusters containing both effectors were detected at fusion sites.

[1]This research project has also been supported by the Investissements d'Avenir programme ANR-11-IDEX-0005-02, Sorbonne Paris Cite, Laboratoire d'excellence INFLAMEX. The research of JR and RS is supported by the intramural research program of the National Institute of Arthritis and Musculoskeletal and Skin Diseases, National Institutes of Health. This work was also supported by the COST Action BM1007 (Mast cell and basophils–targets for innovative therapies) of the European Community. The research project of UB and CB has also been supported by a Marie Curie Early Stage Research Training Fellowship of the European Community's Sixth Framework Programme under contract number 504926 and by the Fondation de Recherche Médicale.

[6]Abbreviations used in this paper: SNARE, N-ethylmaleimide-sensitive factor attachment protein receptors; MC, mast cell; STX, Syntaxin; SG, secretory geranule; PM, plasma membrane; BMMC, bone marrow derived mast cells; RPMC, rat peritoneal mast cells

[5] To whom correspondence should be addressed: Ulrich Blank, INSERM U699, Faculté de Médecine X. Bichat, 16 rue Henri Huchard, 75780 Paris Cedex 18. Tel +33 (0)1 57 27 73 45, Fax: +33 (0)1 57 27 76 61, ulrich.blank@inserm.fr.
[3]Present address: CMU Department of Cellular Physiology and Metabolism, School of Medicine, University of Geneva, Rue Michel Servet, 1, 1211 Geneva 4, Switzerland
[4]Present address: Aix-Marseille University, Assistance Publique Hopitaux de Marseille, Laboratoire d'Immunologie, 13005, Marseille, France

In resting cells, Munc18-2, but not STX3, interacted with tubulin. This interaction was sensitive to nocodazole treatment and decreased after stimulation. Our results indicate that Munc18-2 dynamically couples the membrane fusion machinery to the microtubule cytoskeleton and demonstrate that Munc18-2 and STX3 perform distinct, but complementary, functions to support, respectively, SG translocation and membrane fusion in mast cells.

Introduction

Mast cells (MC) are key effectors in immunity, but are also notoriously known to cause allergies (1). Activation through IgE receptors (FcεRI) triggers degranulation with release of inflammatory mediators stored in abundant cytoplasmic secretory granules (SGs). This is followed by *de novo* synthesis and secretion of cytokines/chemokines (2). In contrast to neuronal/neuroendocrine cell exocytosis, where individual SGs fuse at the plasma membrane (PM), MC degranulation involves granule-granule and SG-PM fusion by compound/multigranular exocytosis (3). Despite these differences, MC and other regulated-secretion competent cells share a common molecular machinery of membrane fusion (2, 4, 5). It includes SNARE fusion (6, 7) and fusion regulatory proteins such as Munc18 (8-10), Munc13 (11, 12), Rab (13-15) complexin (16), SCAMP (17) and Synaptotagmin-family members (18, 19). SNAREs promote fusion by forming a tetrameric complex through their SNARE motif (20). A functional complex in MC comprises the vesicular SNARE (v-SNARE) VAMP8 and the target-SNAREs (t-SNAREs) STX4 and SNAP-23 (6, 7, 21, 22). In agreement with the heterogeneity of the SG compartment and the possibility of granule-granule fusion, other SNAREs may also play a role (9, 23-25). During degranulation, SNAP-23 redistributes from the PM into nascent degranulation channels, which may be a particularity of compound exocytosis (6).

Mammalian homologs of *Caenorhabditis elegans* uncoordinated-18 (Munc18) proteins are essential regulators of exocytosis as evidenced after genetic deletion of the neuronal isoform Munc18-1 (20) and the more ubiquitously expressed isoforms Munc18-2 and Munc18-3 (10, 26-28). Their action involves different SNARE binding modes (20, 29, 30). While binding to the “closed” conformation of Syntaxin was thought to block SNARE assembly (31), new evidences rather support that this complex serves as an “organizer” of productive membrane fusion allowing privileged interactions with other fusion effectors and the promotion of a conformational switch to an “open” form (20) able to bind tetrameric SNARE complexes at its C-terminus thereby activating fusion (30, 32, 33). Although this defines a minimal fusion entity (32), additional evidence indicates that in living cells Munc18 proteins participate in steps promoting vesicle translocation, tethering and docking that are required to support fusion (29).

MC express the ubiquitous isoforms Munc18-2 and Munc18-3 (8). Multiple studies support a role for Munc18-2 in degranulation (8-10, 34, 35). Furthermore, familial hemophagocytic lymphohistiocytosis type 5 (FHL-5) patients carrying Munc18-2 mutations causing misfolding show impaired lytic granule exocytosis in natural killer and cytotoxic T cells (36, 37). In contrast to other immune effector cells (34, 38, 39), a role for PM-localized Munc18-3 in MC has not been demonstrated and the implication of the neuronal specific Munc18-1 is controversial (35, 40)

The cytoskeleton also plays an important role in vesicular trafficking. MC activation is accompanied by cortical actin disassembly and membrane ruffling that favors access of SGs to the PM (41-43). Similarly the actin regulatory proteins coronin 1a/b have recently been shown to differentially effect on degranulation and cytokine production (44). FcεRI

stimulation also triggers microtubule formation through a Fyn/Gab2/RhoA signaling pathway necessary for SG translocation (43, 45).

Here we investigated the role of Munc18-2 and STX3 in degranulation. We show that they have essential but complementary roles and define a new stimulatory Munc18-2 microtubule-dependent axis enabling SG translocation and fusion.

Materials and Methods

Reagents and antibodies

Rabbit Abs to STX3, Munc18-2, rabbit isotype control anti-GST, mouse isotype control IgG (15.1) and mouse monoclonal anti-DNP-IgE have been described (8, 22, 46). Anti-α-tubulin, DNP-human serum albumin (DNP_{30-40}-HSA, Ag), ionomycin, Phorbol 12-myristate 13-acetate (PMA) were purchased from Sigma-Aldrich. Alexa Fluor 555-wheat germ agglutinin (WGA) was from Invitrogen. Murine IL-3 and SCF were from PeproTech (Paris, France). Nocodazole and Paclitaxel were purchased from Merck-Calbiochem (Nottingham, UK).

Cell lines, primary mast cell cultures and preparation of peritoneal mast cells

The rat RBL-2H3 mast cell line and COS7 cells were maintained as described (8, 22, 46). Bone marrow was isolated from femurs of C57/BL6 mice (8-12-wk-old) and BMMC were derived as described (22). Cell cultures were used after 4-8 weeks after routine checking for purity by evaluating expression of c-kit and FcεRI (6, 22). Wistar male or female rats (200 to 400g) were purchased from the University of Trieste. Rats were euthanized by CO_2 inhalation. Rat peritoneal mast cells (RPMC) were obtained and stimulated using compound 48/80 as described (22). All animal studies have been approved by the local institutional animal care and use committees.

Gene modifications in RBL-2H3 cells and BMMC

The following siRNAs (sense) were used (Eurogentec, Belgium): Munc18-2-siRNA1 (GGCUCAUCGUGUACAUUG); Munc18-2-siRNA2 (CGCUCACAGUUGCUCAUAA); STX3-siRNA1 (GGCUCAACAUCGACAAGAU), sSTX3-siRNA2 (GGAGCUCCAUGACAUGUUU); universal scramble siRNA GCCCCGUCUACAUACAUGU. RBL cells were transfected with annealed siRNAs (0.05 μM each) in two successive electroporations 24 h apart adjusting cell density each time to 1×10^7/ml in electropermeabilization buffer (120 mmol/L KCl, 10 mmol/L NaCl, 1 mmol/L KH_2PO_4, 10 mmol/L glucose, 20 mmol/L Hepes, pH 7.0) at 250 V and 2100 μF. Cells were used for functional analysis the next day. For gene silencing of BMMC, shRNA targeting of Munc 18-2 or STX3 was performed using lentiviral vectors. Viruses were produced by transfecting vectors with Munc18-2 or STX3 shRNAs into the packaging cells 293LTV using Lipofectamine 2000 (Invitrogen) as described (47). For infection, 10 day old-bone marrow cells were resuspended in the concentrated viral supernatants for 2 days at 37°C with 5% CO_2. After infection, cells were grown in IL-3- and SCF-containing medium for 2 days before initiating selection of transduced cells with 8 μg/ml blasticidinS (Invitrogen) for two weeks. For transient expression of CD63-GFP, Nucleofection (Amaxa) was performed according to the manufacturer's instructions using mouse macrophage nucleofection program. BMMCs were cultured in IL-3- and SCF-containing medium for 2 days until experiments.

Degranulation measurements and determination of CCL-2 production

Release of granule content was determined by measuring β-hexosaminidase release (7). CCL2 release was quantified using a Duoset cytokine ELISA kit (R&D Systems, France).

Degranulation of BMMC was evaluated by a CD63 expression assay. Briefly, BMMC were deprived of SCF overnight followed by sensitization with DNP-specific IgE in Tyrode's buffer (7) for 3 h at 37°C. IgE-sensitized BMMCs (2×10^6 cells) or unsensitized BMMCs were stimulated with DNP-HSA (Ag) or PMA/ionomycin (20ng/ml 1μM) for 30 min at 37°C. Cells were incubated with anti-CD63 antibodies (2μg/mL, MBL International) or isotype control (2 μg/mL) at 4°C followed by incubation with Alexa Fluor 488 conjugated anti-rat IgG before analysis by flow cytometry using a FACSCalibur (BD Biosciences, San Jose, CA) and FlowJo software (Treestar Inc., Ashland, OR).

Immunoblotting and immunoprecipitation

IgE-sensitized or unsensitized RBL cells (1×10^7) were resuspended in medium and challenged with Ag (DNP-HSA, 100 ng/ml) or PMA/ionomycin (20 nM/1μM) for the indicated times. Stimulation was arrested using ice-cold PBS. Lysates were prepared in 50 mM HEPES pH7.3 containing 10 mM CHAPS, 0.1 % SDS, 150 mM NaCl, 5 mM KCl, 1 mM $MgCl_2$, 1 mM sodium orthovanadate and protease inhibitors as described (6, 22) and used for Munc18-2-tubulin co-immunoprecipitation studies. Munc18-2-STX3 interactions were explored using BMMC (48h). After washing, IgE-sensitized cells were resuspended in medium and challenged with DNP-HSA (10 ng/ml). Stimulation was arrested using ice-cold PBS containing 0.25 mM N-ethylmaleimide (NEM) for 15 min followed by a wash in PBS. Lysates were prepared in 50 mM HEPES pH7.2 containing 1 % Triton X100, 150 mM NaCl, 5 mM KCl, 1 mM $MgCl_2$, 1 mM sodium orthovanadate and protease inhibitors before immunoprecipitation. Immunoblotting was carried out as previously described (22, 47).

Confocal microscopy

siRNA-transfected RBL cells were seeded in 24-well plates on coverslips for 16 h at 37°C in a humidified atmosphere with 5% CO_2. After PMA/ionomycin stimulation, cells were washed and fixed for 20 min on ice in 10 mM PIPES pH6.8, 150 mM NaCl, 5 mM EGTA, 5mM $MgCl_2$, 5 mM glucose containing 4% paraformaldehyde (IF buffer) followed by 2 washes in IF buffer. Fixed cells were permeabilized in IF buffer containing 0.025% saponin for 20 min at room temperature, followed by blocking in IF buffer containing 0.012% saponin and 7% horse serum (Invitrogen) for 30 min at room temperature (RT). Staining with primary Abs was performed in IF buffer containing 0.012% saponin and 5% horse serum for 2 h at RT followed by incubation with secondary Abs for 60 min at RT. Cells were mounted in Prolong-Gold anti-fading reagent (Molecular Probes) and were analyzed using confocal laser-scanning microscope LSM 510, Zeiss (Oberkochen, Germany).

Real time imaging of CD63-GFP expressing granules

For real time imaging of secretory granules, CD63-GFP expressing granules were tracked. CD63-GFP transduced BMMCs were incubated with Alexa Fluor 555-wheat germ agglutinin (5 μg/mL) and placed on poly-d-lysine coated glass bottom dishes for 10 min at 37 °C. Cells were washed, and subsequently stimulated with PMA/ionomycin (20 nM/1μM). A Zeiss LSM-510 META confocal microscope with 488-nm and 543-nm wavelength light from an argon laser and HeNe were used for SG-PM colocalization measurements. The fluorescence of GFP and Alexa Fluor 555 were detected through a band pass filter (505-530 nm) and a long pass filter (>560 nm), respectively. Fluorescence images were collected every 2 s and the acquired data were processed by the Adobe Photoshop. Colocalization coefficient analysis was made using Medical Image Processing Analysis and Visualization (MIPAV, NIH) software. Data of colocalization coefficient were normalized to the starting point (t=0). Increase of value indicates SG-PM membrane fusion. Imaris software (Bitplane AG, Zurich, Switzerland) was used for tracking of CD63-GFP expressed SG and for analyzing granule velocities by the spot-detection function using the following parameters:

autoregressive motion, gapclose 2, 2 μm maximum distance. Average velocities of each granule were analyzed before (1-20 frames) and after (21-50 frames) stimulation.

Electron microscopy

Double immunogold labeling of rat peritoneal mast cells (RPMC) ultrathin sections was as described before (22, 34). Briefly, RMPC were fixed in 1.5% glutaraldehyde (Serva) diluted in 0.1M cacodylate buffer, pH 7.4 stored for 20 min at room temperature, post-fixed in 1% OsO_4 for 60 min at 4°C, dehydrated in ethanol, and finally embedded in Dow Epoxy Resin (DER 332, Unione Chimica Europea, Milano, Italy). For double immunogold labelling ultrathin sections, cut by an ultramicrotome (Ultracut UCT; Leica, Wien, Austria) were mounted on nickel grids etched for one min with 1% periodic acid and rinsed in distilled water three times (2 min each time). The grids with the section sides facing downward were incubated in 20 mM Tris-HCl pH 8.2, containing 2%BSA,1% goat serum,0.05% tween-20 and 0.1%Triton X-100 containing rabbit anti-Munc18-2 (50 μg/ml) at 4°C overnight. After washing in 20 mM Tris-HCl pH 8.2 containing NaCl 225 mM, 20mM NaN3, 0.05% tween-20, 0.5%BSA, 0.1%Triton-X-100, goat serum 0.5% grids were incubated for 1h at room temperature with 10 nm gold-conjugated goat anti-rabbit (British Biocell International; Cardiff, UK) diluted 1:50 in Tris-HCl-BSA-Triton. After rinsing thoroughly, grids were turned over with the section sides facing upward, according to Bendayan (48) and exposed to rabbit anti-STX3 (50 μg/ml) The procedure followed thereafter was as described above with the exception that 20nm gold-conjugated protein A-G (British Biocell International) diluted 1:50 in Tris-HCl-BSA-Triton was used as revealing system. Sections were analyzed by a Philips EM208 transmission electron mmicroscope mounted to a 4008 × 2672 pixel Morada camera (Olympus). Control experiments using irrelevant IgG performed in parallel showed no significant immunogold labeling.

Statistical Analysis

Results were analysed using GraphPad Prism (GraphPad Software Inc, California, USA). Statistical analysis of differences between groups was determined by unpaired, two-tailed student's *t*-tests or by one-way ANOVA as appropriate. Two-way ANOVA was used to examine the overall effects of phenotype and time on the changes in granule-plasma membrane colocalization. Differences were considered significant if the p value was ≤ 0.05 with the confidence intervals of 95%.

Results

Munc 18-2 and STX3 have independent roles and complement in MC degranulation

We explored the role of Munc18-2 in mast cell secretory responses by siRNA-mediated silencing in RBL-2H3 mast cells. Munc18-2 expression was downregulated in RBL MC using siRNA. Consistent with the extent of specific knock-down (Fig.1A), IgE-induced release of the granule-stored enzyme β-hexosaminidase was diminished (Fig.1B). RNA silencing of the Munc18-2 interacting partner and SG-localized SNARE protein STX3 (Fig. 1C) also inhibited IgE-induced degranulation with two independent siRNAs (Fig.1D and data not shown). Interestingly, combined silencing of STX3 and Munc18-2 resulted in an additive inhibitory effect (Fig.1D) demonstrating that they can contribute to degranulation independently of each other. Degranulation was also inhibited after stimulation with PMA/ionomycin (Fig. 1D), which bypasses early FcεRI-induced signaling, supporting the view that both effectors function in the late steps of stimulus-secretion coupling. This is also supported by data showing that more upstream responses such as calcium mobilization were not affected (not shown). No effect of Munc18-2 silencing on STX3 and Munc18-3 expression was observed (Fig.1C and data not shown). This excludes a chaperon function of Munc18-2 for STX3 as observed for other Munc18 binding proteins (36, 49). We also

analyzed the effect on *de novo* CCL2 chemokine secretion. Neither silencing of Munc18-2 or of STX3, nor a combined knock-down of both affected IgE-induced CCL2 release when compared to cells transfected with scrambled siRNA (Fig.1E). As STX3 has not been previously implicated in mast cell degranulation (7), we evaluated the respective contribution of STX3 and STX4 in the degranulation response. Surprisingly, siRNA experiments (Fig. S1) showed that the effect of STX3 silencing was more pronounced than that of STX4. No additive effect was observed when both STXs were downregulated.

Silencing of Munc18-2 expression restricts SG translocation and fusion

To explore the mechanism of action of Munc18-2, in mast cells we investigated the consequences of silencing its expression on the location of SGs in resting and stimulated RBL mast cells. SGs were labeled with an Ab to STX3 (a SG resident protein) and their distribution was compared to microtubules, based on findings that SGs are mobilized along microtubules (8, 43, 45). Fig. 2 shows that in resting, siRNA controls, SGs (in green) are randomly distributed along microtubules (in red) and often concentrate around the MTOC or in proximity to the PM (Fig.2, upper left panel). This distribution was not altered in Munc18-2-silenced cells (Fig.2, lower left panel). PMA/ionomycin stimulation of control siRNA treated cells induced the formation of microtubular tracks reaching out to the plasma membrane into filopodia-like extensions in (Fig. 2, upper right panels). At the same time SGs aligned along these tracks and substantial STX3 immunolabeling was observed at the periphery indicating that SGs had translocated and fused with the PM. Similar data were also obtained when cells were stimulated with IgE/Ag albeit STX membrane translocation was somewhat less prominent as compared to PMA/ionomycin-stimulated cells (Fig. S2). Munc18-2 silencing did not affect microtubule formation (Fig.2 lower right panel), however, SG movement to the periphery was markedly altered with most SG remaining in the cytosol, although they remain attached to microtubules. This indicated that the inhibitory effect on degranulation in the absence of Munc18-2 was due to the inhibition of SG translocation and subsequent incorporation into the PM.

To further confirm and extend these findings, we used dynamic image analysis of primary bone marrow derived MC (BMMC) after silencing the expression of Munc18-2 or its binding partner STX3. Cells were transduced with lentiviruses encoding shRNAs corresponding to Munc18-2 (shMunc18-2), STX3 (shSTX3) or scrambled controls (shScr). Fig. 3A shows that partial but specific silencing of Munc18-2 or STX3 was achieved when compared to WT or scrambled control shRNA. Like in RBL cells, silencing of STX3 had no effect on Munc18-2 expression or *vice versa*. Viral transduction also did not affect expression levels of FcεRI or the general phenotype or growth properties of these cells (Fig. 3B and data not shown). As observed before in RBL cells, silencing of Munc18-2 or STX3 markedly diminished cell surface expression of CD63 (a surrogate marker of mast cell degranulation at the PM) after IgE/Ag or PMA/ionomycin-induced degranulation when compared to WT or control shRNA-transduced cells (Fig 3C-E). Release of granule-stored β-hexosaminidase was similarly inhibited (Fig. S3). To follow SG movement and SG fusion events with the PM in real-time, we additionally transfected cells with CD63-GFP, which incorporates into mast cell SGs (43). The PM was labeled by loading cells with Alexa Fluor 555-conjugated wheat-germ agglutinin and cells were then stimulated using PMA/ ionomycin. The dynamics of SG movement and their tracking using real-time CD63-GFP imaging analysis are shown in Movies S1A-S1D. Representative images of the monitored fusion events during time (yt and xt) as compared to the xy image at the beginning and end of the stimulation period are depicted in Fig. 4A. In WT (Fig. 4A (WT), Movie S1A) or control shRNA-treated BMMC (Fig.4A (19D), Movie S1B), SGs became highly mobile and moved towards the PM (open arrowhead in Fig 4A (WT, 19D)). Velocities of these SGs were increased after stimulation (Fig 4B (WT) and (19D)). Furthermore, SGs and PM fusion

were observed in WT or control shRNA-treated BMMC (arrows in Fig 4A (WT, 19D)). Following specific silencing of either Munc18-2 or STX3, SGs showed distinct features and differential behavior when compared to control-treated or WT BMMCs. When Munc18-2 was silenced (Fig 4A (23B), Movie S1C), SGs lose their direction and move randomly in the cytosol (open arrowhead). In addition, SGs in Munc18-2 silenced BMMCs showed strongly reduced velocities compared with WT or 19D controls. Conversely, silencing of STX3 (Fig 4A (16B), Movie S1D) showed that SGs remained highly mobile, yet upon reaching the PM they rarely fused (indicated by the arrow head in Fig 4A (16B)). To quantify the occurring fusion events we measured colocalization of SG and PM markers as a function of time by correlation coefficient analysis (Fig. 4C). An increase in value indicates improved fusion of CD63-GFP positive granules with the PM. The number of fusion events in WT and control shRNA transduced cells rapidly rose to a maximum before starting to decline at the end of the monitoring period. In Munc18-2 silenced cells a small rise in fusion events was observed, however, this rise was delayed and was minor relative to control cells. Importantly, due to the decreased and random mobility of CD63-GFP positive granules, fewer SGs reached the PM (Fig 4A and 4B). In contrast, STX3 silencing showed that, although CD63-GFP positive SGs were observed in close proximity to the PM, fusion events were diminished.

Microtubule dependent regulation of Munc18-2 function during stimulation

During analysis of SG dynamics, we noticed that in some instances SGs remained immobile in areas that appeared to be restricted or relatively sparse in microtubular networks, while they readily moved and fused in other areas (Movie S2). This argued for the need of cytoskeletal reorganization to coordinate SG mobility and fusion. In light of the deficiency in translocation we explored whether Munc18-2 could be part of a complex that couples the SG fusion machinery with microtubules. As shown in Fig. 5A (upper panel) myc-tagged Munc18-2 transfected into COS7 cells was specifically coimmunoprecipitated with α-tubulin. Similarly, endogenous Munc18-2 was found to associate with α-tubulin in RBL MCs (Fig.5A lower panel and Fig. 5B), This association was decreased in cells treated with the microtubule dissolving drug nocodazole (Fig. 5B). We next examined whether the Munc18-2 binding partner STX3 and the non-interacting protein STX4 cognate SNARE fusion proteins also coimmunoprecipitated with tubulin. However, while we confirmed previous data that Munc18-2 interacts with STX3 but not with STX4 or SNAP23 neither of these antibodies was able to co-immunoprecipitate tubulin supporting a Munc18-2-dependent but STX3-independent interaction (Fig. 5C). We further analyzed whether the Munc18-2-tubulin interaction was modulated upon stimulation. Our kinetic analysis showed a time-dependent decrease of the interaction in both IgE/Ag and PMA/Ionomycin stimulated cells (Fig. 5D).

Ultrastructural analysis of Munc18-2 and STX3 localisation and interaction

We next used immunogold labeling and electron microscopy to visualize at the ultrastructural level the distribution of Munc18-2 (10 nm GP) and STX3 (20 nm GP) in rat peritoneal MC (RPMC). The latter contain a highly differentiated granular compartment and upon stimulation release granular content by a process involving both SG-SG fusion and SG-PM fusion. Representative images of the GP distribution in resting and stimulated cells are depicted in Fig.6. Quantitative analysis of GP distribution in resting cells shows that Munc18-2 is majorly (80 %) associated with SGs (Table 1) both on the surface (Fig.6 black arrows in panel A, C, E) but to a large part also inside the matrix (Fig.6 black arrowheads in panel A, E). The latter finding could relate to the fact that mast cell granules and those of other secretory cells have been found to contain exosomes (25, 50). A sizable proportion of Munc18-2 (20 %) was also found in zones connecting SGs each to the other. These connections appeared to be constituted of filamentous tangles that appear attached to

membranous extensions of the SGs (Fig.6 panel A, C thin black arrows). PM localization, although occasionally seen, was rare. Similar to Munc18-2, the majority of STX3 was found on the SGs surface (22.5 %) (Fig.6 panel A, C white arrows) and within SGs (68.1 %) (Fig.6 panel A, E white arrowheads). STX3 was also clustered at sites with filamentous connections (9.4 %) often together with Munc18-2 (Fig.6 panel A thin white arrows). Treatment with microtubule-depolymerizing or-stabilizing drugs induced the disappearance of Munc18-2 and STX3 labeling at the level of the filamentous connection in nocodazol and taxol treated RPMC, respectively (Fig. S4 and Table 1). Quantitation of immunogold labeling also showed that the amount of the granule matrix GP in these cells did not change, while on the average an increase of granule surface labeling was noted (Fig. S4 and Table 1). After stimulation, numerous fusion events with the expansion of the granular matrix can be observed (Fig. 6 panel B). Interestingly, large clusters of STX3 and Munc18-2 can frequently be seen often coinciding with possible sites of fusion between granules (Fig. 6 white arrowheads in panel B and at higher magnification in panels D), but also between granules and the PM (Fig. 6 panel F).

Discussion

Here we report that the SNARE regulator Munc18-2 and its STX3 binding partner have distinct, but complementary roles in MC degranulation. Munc18-2 supports exocytosis by facilitating translocation of SGs, whereas STX3 plays a direct role in fusion. Nonetheless, STX3 function is apparently intimately linked to Munc18-2 as indicated by the observed coclustering at fusion sites in degranulating cells. Our findings also demonstrate that Munc18-2 is coupled to cell signaling, which modulates its interaction with the microtubule cytoskeleton.

Munc18 proteins are essential fusion effectors in regulated exocytosis, however, their precise function remains incompletely understood (20). In addition to their direct fusion promoting role (20, 30), Munc18 proteins were proposed to regulate additional steps such as vesicle translocation, docking, postdocking and modulation of cytoskeletal functions (29, 51, 52). In this line, Munc18-1-deficient chromaffin cells revealed a largely altered distribution of dense core vesicles, attributed to a docking defect (53). The defect was overcome by overexpressing STX1, which prevents formation of “non-productive” SNARE (STX1-STX1-SNAP-25) complexes (53) suggesting that Munc18-1 could serve as an organizer of productive SNARE assembly. This view is also validated by reconstitution experiments (33).

Early studies on the ubiquitously expressed Munc18-2 showed that it controls exocytosis in various epithelial cells (54, 55), amylase release from pancreatic acinar cells (56) or insulin release from pancreatic beta cells (57). Munc18-2 was also implicated in SG release by immune cells including MC and neutrophils (8-10, 34). The discovery of Munc18-2 mutations in immune deficiency FHL-5 patients leading to misfolding were shown to affect STX11 expression and to lead to a defect in lytic granule exocytosis in natural killer (NK) and cytotoxic T cells (CTL)(36, 37). Although these results indicate that Munc18-2, similarly to Munc18-1, plays an important role in regulated secretion, the functions of these two SNARE accessory proteins may not be completely identical. Thus, in MC and other cell types (34, 57), the granular localization of Munc18-2 and STX3 is strikingly different. In epithelial cells, Munc18-2 was associated with polarized secretory events as it was found to regulate - together with STX3 - apical secretion in both intestinal and kidney epithelial cells (54, 55, 58). Interestingly, a recent study performed with pancreatic acinar cells suggested a preponderant role of Munc18-2 in sequential fusion (59). Other differences are the specific binding of calcium EF-hand protein Cab45 to Munc18-2 in the absence of calcium, whereas Munc18-1 binds only in its presence (60). It has been proposed that this interaction, which

occurs in the absence of STX3, might regulate the association of Munc18-2 with STX partners during exocytosis (57).

Concerning mast cells our data show that downregulation of either Munc18-2 or STX3 expression markedly inhibited MC degranulation, while CCL2 chemokine secretion was not affected arguing that both effectors function only in release from storage organelles. These experiments implicate STX3, in addition to STX4 (7, 61, in regulating degranulation. STX11 has also been a potential candidate for regulating mast cell degranulation. However, although STX11 decreases in Munc18-2-deficient mast cells {Bin, 2013 #20183)in regulating degranulation. STX11 has also been a potential candidate for regulating mast cell degranulation. However, although STX11 decreases in Munc18-2-deficient mast cells no effect on degranulation was seen in mast cells from STX11-deficient mice (35, 40), (62). Interestingly STX3 downregulation had a more pronounced effect on degranulation than downregulation of STX4. Given the SG localization of the former, this finding supports the hypothesis that sequential granule-granule fusion is an important contributor in MC degranulation. Nonetheless, STX3 was also found in clusters at the membrane suggesting that during this process it is able to relocate to this compartment in a manner similar to SNAP23, which in a reverse manner relocates from the plasma membrane to SG during degranulation (6). No additive effect on degranulation was observed, when both STX3 and STX4 were simultaneously downregulated suggesting that they function independently. By contrast, inhibitory effects on degranulation were enhanced when Munc18-2 and STX3 expression were jointly reduced suggesting unique, but complementary functions for each protein in this process.

Importantly, confocal imaging and live cell imaging studies of the degranulation process support that Munc18-2 controls granule translocation contrasting with STX3, which as expected directly impacts on fusion. As degranulation involves microtubule-dependent SG transport (43, 45, 63), this suggested that Munc18-2 might play a role in connecting the fusion apparatus with the microtubule cytoskeleton. In support, previous studies have shown that Munc18-2 labeled SG align along microtubules (8). Similarly a sizable proportion of Munc18-2 can be found at cytoskeletal granular connections. Furthermore, neuronal Munc18-1 was shown to bind to the Kinesin-1 adaptor protein “fasciculation and elongation protein zeta-1” (FEZ1) (64) providing a link to axonal-dependent vesicular transport. We therefore asked whether Munc18-2 could interact with microtubules. Using coimmunoprecipitation experiments showed that Munc18-2 associated in a specific manner with α-tubulin. This interaction decreased in the presence of nocodazole. Importantly, the interaction was downmodulated after stimulation suggesting a dynamic coupling during cell signaling. Likely, Munc18-2 is not directly responsible for this interaction, as SGs remain attached to microtubules after Munc18-2 silencing (Fig.2). Likewise, attachment seems to take place independently of Munc18-2 binding to STX3 as tubulin was not found to coimmunoprecipitate with anti-STX3 and specific knockdown of STX3 did not affect the interaction (not shown). However, so far we have been unable to detect interactions of Munc18-2 with other microtubule associated proteins like kinesin or the FEZ1 homologue FEZ2 (not shown). Based on our results that SG translocation is clearly affected, it is possible that Munc18-2 could promote dynamic exchanges between the fusion and the cytoskeletal transport machinery, perhaps by enabling multiple cycles of docking. Likely this could take place independent of its binding to STX3 as also suggested by the additive effect of downregulation of both STX3 and Munc18-2. These data are also in agreement with the described docking defects in Munc18-1 null chromaffin cells (53), but suggest that docking could be a dynamic process involved in granule translocation. In agreement, FHL5 patients carrying mutations in Munc18-2 retain persistent membrane trafficking defects in epithelial cells even after hematopoietic stem cell transplantation with inappropriate accumulation of granules in the cytoplasm similar to what is seen in MC (65).

The importance of microtubules in organizing the cellular distribution of the core fusion machinery is also supported by ultrastructural studies. Munc18-2 GP are found mainly in association with secretory granules confirming our previous data (8), but also labeled granule-connecting filamentous structures. This distribution, in particular those present in the filamentous connections, is decreased in the presence of microtubule targeting drugs supporting the above hypothesis that it could depend on dynamic interactions of Munc18-2 with the microtubule network. This is in agreement with early transmission EM observations in RPMC, which revealed an important cytoskeletal meshwork around SGs and microtubules connecting the SG surface to the subplasmalemmal network or to the adjacent granule surface (66, 67). On some occasions, however, large clusters of both molecules accumulated at sites of granule-granule or granule-PM fusion suggesting that at the fusion site productive interactions are maintained to support fusion. Taken together these data support the important role of the dynamic interactions of the secretory machinery with the cytoskeleton as already shown in the case of Rab3D, that could play a role in actin coating of secretory granules during exocytosis (68, 69) or Rab27 isoforms that could regulate the transition of microtubule to actin based motility of granules (70).

Collectively, our findings establish Munc18-2 as an important regulator of MC prestored mediator release that functions by enhancing SG translocation. Concerning STX3 our findings support a major role in SG-SG and SG-PM fusion. We also define a new Munc18-2-microtubule-dependent regulatory axis that coordinately organizes productive interactions between promoters of SG translocation and fusion with the cytoskeleton.

Supplementary Material

Refer to Web version on PubMed Central for supplementary material.

Acknowledgments

We thank Samira Benadda, IFR-02 for the help with confocal imaging. The research of JR is supported by the intramural research program at NIAMS, NIH.

References

1. Galli SJ, Kalesnikoff J, Grimbaldeston MA, Piliponsky AM, Williams CM, Tsai M. Mast cells as “tunable” effector and immunoregulatory cells: recent advances. Annu Rev Immunol. 2005; 23:749–786. [PubMed: 15771585]
2. Blank U, Rivera J. The ins and outs of IgE-dependent mast-cell exocytosis. Trends Immunol. 2004; 25:266–273. [PubMed: 15099567]
3. Alvarez de Toledo G, Fernandez J. Compound versus multigranular exocytosis in peritoneal cells. J. Gen. Physiol. 1990; 95:397–402. [PubMed: 2324701]
4. Stow JL, Manderson AP, Murray RZ. SNAREing immunity: the role of SNAREs in the immune system. Nat Rev Immunol. 2006; 6:919–929. [PubMed: 17124513]
5. Benhamou M, Blank U. Stimulus-secretion coupling by high-affinity IgE receptor: new developments. FEBS Lett. 2010; 584:4941–4948. [PubMed: 20851120]
6. Guo Z, Turner C, Castle D. Relocation of the t-SNARE SNAP-23 from lamellipodia-like cell surface projections regulates compound exocytosis in mast cells. Cell. 1998; 94:537–548. [PubMed: 9727496]
7. Paumet F, Le Mao J, Martin S, Galli T, David B, Blank U, Roa M. Soluble NSF attachment protein receptors (SNAREs) in RBL-2H3 mast cells: functional role of syntaxin 4 in exocytosis and identification of a vesicle-associated membrane protein 8-containing secretory compartment. J Immunol. 2000; 164:5850–5857. [PubMed: 10820264]

8. Martin-Verdeaux S, Pombo I, Iannascoli B, Roa M, Varin-Blank N, Rivera J, Blank U. Analysis of Munc18-2 compartmentation in mast cells reveals a role for microtubules in granule exocytosis. J. Cell Sci. 2003; 116:325–334. [PubMed: 12482918]
9. Tadokoro S, Kurimoto T, Nakanishi M, Hirashima N. Munc18-2 regulates exocytotic membrane fusion positively interacting with syntaxin-3 in RBL-2H3 cells. Mol Immunol. 2007; 44:3427–3433. [PubMed: 17408745]
10. Kim K, Petrova YM, Scott BL, Nigam R, Agrawal A, Evans CM, Azzegagh Z, Gomez A, Rodarte EM, Olkkonen VM, Bagirzadeh R, Piccotti L, Ren B, Yoon JH, McNew JA, Adachi R, Tuvim MJ, Dickey BF. Munc18b is an essential gene in mice whose expression is limiting for secretion by airway epithelial and mast cells. Biochem J. 2012; 446:383–394. [PubMed: 22694344]
11. Higashio H, Nishimura N, Ishizaki H, Miyoshi J, Orita S, Sakane A, Sasaki T. Doc2 alpha and Munc13-4 regulate Ca(2+) -dependent secretory lysosome exocytosis in mast cells. J Immunol. 2008; 180:4774–4784. [PubMed: 18354201]
12. Neeft M, Wieffer M, de Jong AS, Negroiu G, Metz CH, van Loon A, Griffith J, Krijgsveld J, Wulffraat N, Koch H, Heck AJ, Brose N, Kleijmeer M, van der Sluijs P. Munc13-4 is an effector of rab27a and controls secretion of lysosomes in hematopoietic cells. Mol Biol Cell. 2005; 16:731–741. [PubMed: 15548590]
13. Mizuno K, Tolmachova T, Ushakov DS, Romao M, Abrink M, Ferenczi MA, Raposo G, Seabra MC. Rab27b regulates mast cell granule dynamics and secretion. Traffic. 2007; 8:883–892. [PubMed: 17587407]
14. Pombo I, Martin-Verdeaux S, Iannascoli B, Le Mao J, Deriano L, Rivera J, Blank U. IgE receptor type I-dependent regulation of a Rab3D-associated kinase: a possible link in the calcium-dependent assembly of SNARE complexes. J Biol Chem. 2001; 276:42893–42900. [PubMed: 11555639]
15. Azouz NP, Matsui T, Fukuda M, Sagi-Eisenberg R. Decoding the regulation of mast cell exocytosis by networks of Rab GTPases. J Immunol. 2012; 189:2169–2180. [PubMed: 22826321]
16. Tadokoro S, Nakanishi M, Hirashima N. Complexin II facilitates exocytotic release in mast cells by enhancing Ca2+ sensitivity of the fusion process. J Cell Sci. 2005; 118:2239–2246. [PubMed: 15870114]
17. Guo Z, Liu L, Cafiso D, Castle D. Perturbation of a very late step of regulated exocytosis by a secretory carrier membrane protein (SCAMP2)-derived peptide. J Biol Chem. 2002; 277:35357–35363. [PubMed: 12124380]
18. Baram D, Mekori YA, Sagi-Eisenberg R. Synaptotagmin regulates mast cell functions. Immunol Rev. 2001; 179:25–34. [PubMed: 11292024]
19. Melicoff E, Sansores-Garcia L, Gomez A, Moreira DC, Datta P, Thakur P, Petrova Y, Siddiqi T, Murthy JN, Dickey BF, Heidelberger R, Adachi R. Synaptotagmin-2 controls regulated exocytosis but not other secretory responses of mast cells. J Biol Chem. 2009; 284:19445–19451. [PubMed: 19473977]
20. Rizo J, Sudhof TC. The membrane fusion enigma: SNAREs, Sec1/Munc18 proteins, and their accomplices--guilty as charged? Annu Rev Cell Dev Biol. 2012; 28:279–308. [PubMed: 23057743]
21. Puri N, Roche PA. Mast cells possess distinct secretory granule subsets whose exocytosis is regulated by different SNARE isoforms. Proc Natl Acad Sci U S A. 2008; 105:2580–2585. [PubMed: 18250339]
22. Tiwari N, Wang CC, Brochetta C, Ke G, Vita F, Qi Z, Rivera J, Soranzo MR, Zabucchi G, Hong W, Blank U. VAMP-8 segregates mast cell-preformed mediator exocytosis from cytokine trafficking pathways. Blood. 2008; 111:3665–3674. [PubMed: 18203950]
23. Hibi T, Hirashima N, Nakanishi M. Rat basophilic leukemia cells express syntaxin-3 and VAMP-7 in granule membranes. Biochem Biophys Res Commun. 2000; 271:36–41. [PubMed: 10777677]
24. Sander LE, Frank SP, Bolat S, Blank U, Galli T, Bigalke H, Bischoff SC, Lorentz A. Vesicle associated membrane protein (VAMP)-7 and VAMP-8, but not VAMP-2 or VAMP-3, are required for activation-induced degranulation of mature human mast cells. Eur J Immunol. 2008; 38:855–863. [PubMed: 18253931]

25. Raposo G, Tenza D, Mecheri S, Peronet R, Bonnerot C, Desaymard C. Accumulation of major histocompatibility complex class II molecules in mast cell secretory granules and their release upon degranulation. Mol Biol Cell. 1997; 8:2631–2645. [PubMed: 9398681]
26. Oh E, Spurlin BA, Pessin JE, Thurmond DC. Munc18c heterozygous knockout mice display increased susceptibility for severe glucose intolerance. Diabetes. 2005; 54:638–647. [PubMed: 15734838]
27. Kanda H, Tamori Y, Shinoda H, Yoshikawa M, Sakaue M, Udagawa J, Otani H, Tashiro F, Miyazaki J, Kasuga M. Adipocytes from Munc18c-null mice show increased sensitivity to insulin-stimulated GLUT4 externalization. J Clin Invest. 2005; 115:291–301. [PubMed: 15690082]
28. Jewell JL, Oh E, Thurmond DC. Exocytosis mechanisms underlying insulin release and glucose uptake: conserved roles for Munc18c and syntaxin 4. Am J Physiol Regul Integr Comp Physiol. 2010; 298:R517–531. [PubMed: 20053958]
29. Burgoyne RD, Barclay JW, Ciufo LF, Graham ME, Handley MT, Morgan A. The functions of Munc18-1 in regulated exocytosis. Ann N Y Acad Sci. 2009; 1152:76–86. [PubMed: 19161378]
30. Xu Y, Su L, Rizo J. Binding of Munc18-1 to synaptobrevin and to the SNARE four-helix bundle. Biochemistry. 2010; 49:1568–1576. [PubMed: 20102228]
31. Schollmeier Y, Krause JM, Kreye S, Malsam J, Sollner TH. Resolving the Function of Distinct Munc18-1/SNARE Protein Interaction Modes in a Reconstituted Membrane Fusion Assay. J Biol Chem. 2011; 286:30582–30590. [PubMed: 21730064]
32. Shen J, Rathore SS, Khandan L, Rothman JE. SNARE bundle and syntaxin N-peptide constitute a minimal complement for Munc18-1 activation of membrane fusion. J Cell Biol. 2010; 190:55–63. [PubMed: 20603329]
33. Ma C, Su L, Seven AB, Xu Y, Rizo J. Reconstitution of the vital functions of Munc18 and Munc13 in neurotransmitter release. Science. 2013; 339:421–425. [PubMed: 23258414]
34. Brochetta C, Vita F, Tiwari N, Scandiuzzi L, Soranzo MR, Guerin-Marchand C, Zabucchi G, Blank U. Involvement of Munc18 isoforms in the regulation of granule exocytosis in neutrophils. Biochim Biophys Acta. 2008; 1783:1781–1791. [PubMed: 18588921]
35. Bin NR, Jung CH, Piggott C, Sugita S. Crucial role of the hydrophobic pocket region of Munc18 protein in mast cell degranulation. Proc Natl Acad Sci U S A. 2013; 110:4610–4615. [PubMed: 23487749]
36. Cote M, Menager MM, Burgess A, Mahlaoui N, Picard C, Schaffner C, Al-Manjomi F, Al-Harbi M, Alangari A, Le Deist F, Gennery AR, Prince N, Cariou A, Nitschke P, Blank U, El-Ghazali G, Menasche G, Latour S, Fischer A, de Saint Basile G. Munc18-2 deficiency causes familial hemophagocytic lymphohistiocytosis type 5 and impairs cytotoxic granule exocytosis in patient NK cells. J Clin Invest. 2009; 119:3765–3773. [PubMed: 19884660]
37. Zur Stadt U, Rohr J, Seifert W, Koch F, Grieve S, Pagel J, Strauss J, Kasper B, Nurnberg G, Becker C, Maul-Pavicic A, Beutel K, Janka G, Griffiths G, Ehl S, Hennies HC. Familial hemophagocytic lymphohistiocytosis type 5 (FHL-5) is caused by mutations in Munc18-2 and impaired binding to syntaxin 11. Am J Hum Genet. 2009; 85:482–492. [PubMed: 19804848]
38. Schraw TD, Lemons PP, Dean WL, Whiteheart SW. A role for Sec1/Munc18 proteins in platelet exocytosis. Biochem J. 2003; 374:207–217. [PubMed: 12773094]
39. Houng A, Polgar J, Reed GL. Munc18-syntaxin complexes and exocytosis in human platelets. J Biol Chem. 2003; 278:19627–19633. [PubMed: 12649283]
40. Wu Z, Macneil AJ, Berman JN, Lin TJ. Syntaxin Binding Protein 1 Is Not Required for Allergic Inflammation via IgE-Mediated Mast Cell Activation. PLoS One. 2013; 8:e58560. [PubMed: 23484036]
41. Tolarova H, Draberova L, Heneberg P, Draber P. Involvement of filamentous actin in setting the threshold for degranulation in mast cells. Eur J Immunol. 2004; 34:1627–1636. [PubMed: 15162432]
42. Holowka D, Sheets ED, Baird B. Interactions between Fc(epsilon)RI and lipid raft components are regulated by the actin cytoskeleton. J Cell Sci. 2000; 113(Pt 6):1009–1019. [PubMed: 10683149]
43. Nishida K, Yamasaki S, Ito Y, Kabu K, Hattori K, Tezuka T, Nishizumi H, Kitamura D, Goitsuka R, Geha RS, Yamamoto T, Yagi T, Hirano T. Fc{epsilon}RI-mediated mast cell degranulation

requires calcium-independent microtubule-dependent translocation of granules to the plasma membrane. J Cell Biol. 2005; 170:115–126. [PubMed: 15998803]

44. Foger N, Jenckel A, Orinska Z, Lee KH, Chan AC, Bulfone-Paus S. Differential regulation of mast cell degranulation versus cytokine secretion by the actin regulatory proteins Coronin1a and Coronin1b. J Exp Med. 2011; 208:1777–1787. [PubMed: 21844203]
45. Smith AJ, Pfeiffer JR, Zhang J, Martinez AM, Griffiths GM, Wilson BS. Microtubule-dependent transport of secretory vesicles in RBL-2H3 cells. Traffic. 2003; 4:302–312. [PubMed: 12713658]
46. Pfirsch-Maisonnas S, Aloulou M, Xu T, Claver J, Kanamaru Y, Tiwari M, Launay P, Monteiro RC, Blank U. Inhibitory ITAM signaling traps activating receptors with the phosphatase SHP-1 to form polarized “inhibisome” clusters. Sci Signal. 2011; 4:ra24. [PubMed: 21505186]
47. Furumoto Y, Brooks S, Olivera A, Takagi Y, Miyagishi M, Taira K, Casellas R, Beaven MA, Gilfillan AM, Rivera J. Cutting Edge: Lentiviral short hairpin RNA silencing of PTEN in human mast cells reveals constitutive signals that promote cytokine secretion and cell survival. J Immunol. 2006; 176:5167–5171. [PubMed: 16621980]
48. Bendayan M. Double immunocytochemical labeling applying the protein A-gold technique. J Histochem Cytochem. 1982; 30:81–85. [PubMed: 6172469]
49. Bryant NJ, James DE. Vps45p stabilizes the syntaxin homologue Tlg2p and positively regulates SNARE complex formation. EMBO J. 2001; 20:3380–3388. [PubMed: 11432826]
50. Palmisano G, Jensen SS, Le Bihan MC, Laine J, McGuire JN, Pociot F, Larsen MR. Characterization of membrane-shed microvesicles from cytokine-stimulated beta-cells using proteomics strategies. Mol Cell Proteomics. 2012; 11:230–243. [PubMed: 22345510]
51. Kurps J, de Wit H. The role of Munc18-1 and its orthologs in modulation of cortical F-actin in chromaffin cells. J Mol Neurosci. 2012; 48:339–346. [PubMed: 22535313]
52. Meijer M, Burkhardt P, de Wit H, Toonen RF, Fasshauer D, Verhage M. Munc18-1 mutations that strongly impair SNARE-complex binding support normal synaptic transmission. EMBO J. 2012; 31:2156–2168. [PubMed: 22446389]
53. de Wit H, Walter AM, Milosevic I, Gulyas-Kovacs A, Riedel D, Sorensen JB, Verhage M. Synaptotagmin-1 docks secretory vesicles to syntaxin-1/SNAP-25 acceptor complexes. Cell. 2009; 138:935–946. [PubMed: 19716167]
54. Kauppi M, Wohlfahrt G, Olkkonen VM. Analysis of the Munc18bsyntaxin binding interface. Use of a mutant Munc18b to dissect the functions of syntaxins 2 and 3. J Biol Chem. 2002; 277:43973–43979. [PubMed: 12198139]
55. Nicoletta JA, Ross JJ, Li G, Cheng Q, Schwartz J, Alexander EA, Schwartz JH. Munc-18-2 regulates exocytosis of H(+)-ATPase in rat inner medullary collecting duct cells. Am J Physiol Cell Physiol. 2004; 287:C1366–1374. [PubMed: 15240346]
56. Fukuda M, Imai A, Nashida T, Shimomura H. Slp4-a/granuphilin-a interacts with syntaxin-2/3 in a Munc18-2-dependent manner. J Biol Chem. 2005; 280:39175–39184. [PubMed: 16186111]
57. Zhang Y, Kang YH, Chang N, Lam PP, Liu Y, Olkkonen VM, Gaisano HY. Cab45b, a Munc18b-interacting partner, regulates exocytosis in pancreatic beta-cells. J Biol Chem. 2009; 284:20840–20847. [PubMed: 19487699]
58. Sharma N, Low SH, Misra S, Pallavi B, Weimbs T. Apical targeting of syntaxin 3 is essential for epithelial cell polarity. J Cell Biol. 2006; 173:937–948. [PubMed: 16785322]
59. Lam PP, Ohno M, Dolai S, He Y, Qin T, Liang T, Zhu D, Kang Y, Liu Y, Kauppi M, Xie L, Wan WC, Bin NR, Sugita S, Olkkonen VM, Takahashi N, Kasai H, Gaisano HY. Munc18b is a major mediator of insulin exocytosis in rat pancreatic beta-cells. Diabetes. 2013
60. Lam PP, Hyvarinen K, Kauppi M, Cosen-Binker L, Laitinen S, Keranen S, Gaisano HY, Olkkonen VM. A cytosolic splice variant of Cab45 interacts with Munc18b and impacts on amylase secretion by pancreatic acini. Mol Biol Cell. 2007; 18:2473–2480. [PubMed: 17442889]
61. Woska JR Jr. Gillespie ME. Small-interfering RNA-mediated identification and regulation of the ternary SNARE complex mediating RBL-2H3 mast cell degranulation. Scand J Immunol. 2011; 73:8–17. [PubMed: 21128998]
62. D'Orlando O, Zhao F, Kasper B, Orinska Z, Muller J, Hermans-Borgmeyer I, Griffiths GM, Zur Stadt U, Bulfone-Paus S. Syntaxin 11 is required for NK and CD8(+) T-cell cytotoxicity and neutrophil degranulation. Eur J Immunol. 2013; 43:194–208. [PubMed: 23042080]

63. Cruse G, Beaven MA, Ashmole I, Bradding P, Gilfillan AM, Metcalfe DD. A Truncated Splice-Variant of the FcepsilonRIbeta Receptor Subunit Is Critical for Microtubule Formation and Degranulation in Mast Cells. Immunity. 2013

64. Chua JJ, Butkevich E, Worseck JM, Kittelmann M, Gronborg M, Behrmann E, Stelzl U, Pavlos NJ, Lalowski MM, Eimer S, Wanker EE, Klopfenstein DR, Jahn R. Phosphorylation-regulated axonal dependent transport of syntaxin 1 is mediated by a Kinesin-1 adapter. Proc Natl Acad Sci U S A. 2012; 109:5862–5867. [PubMed: 22451907]

65. Stepensky P, Bartram J, Barth TF, Lehmberg K, Walther P, Amann K, Philips AD, Beringer O, Zur Stadt U, Schulz A, Amrolia P, Weintraub M, Debatin KM, Hoenig M, Posovszky C. Persistent defective membrane trafficking in epithelial cells of patients with familial hemophagocytic lymphohistiocytosis type 5 due to STXBP2/MUNC18-2 mutations. Pediatr Blood Cancer. 2013

66. Nielsen EH, Jahn H. Cytoskeletal studies on Lowicryl K4M embedded and Affi-Gel 731 attached rat peritoneal mast cells. Virchows Arch B Cell Pathol Incl Mol Pathol. 1984; 45:313–323. [PubMed: 6146222]

67. Tasaka K, Akagi M, Mio M, Miyoshi K, Aoki I. The existence of filaments connecting the granules and the cell membrane in rat peritoneal mast cells. Agents Actions. 1991; 33:48–52. [PubMed: 1897447]

68. Valentijn JA, Valentijn K, Pastore LM, Jamieson JD. Actin coating of secretory granules during regulated exocytosis correlates with the release of rab3D. Proc Natl Acad Sci U S A. 2000; 97:1091–1095. [PubMed: 10655489]

69. Coppola T, Perret-Menoud V, Gattesco S, Magnin S, Pombo I, Blank U, Regazzi R. The death domain of Rab3 guanine nucleotide exchange protein in GDP/GTP exchange activity in living cells. Biochem J. 2002; 362:273–279. [PubMed: 11853534]

70. Singh RK, Mizuno K, Wasmeier C, Wavre-Shapton ST, Recchi C, Catz SD, Futter C, Tolmachova T, Hume AN, Seabra MC. Distinct and opposing roles for Rab27a/Mlph/MyoVa and Rab27b/Munc13-4 in mast cell secretion. FEBS J. 2013; 280:892–903. [PubMed: 23281710]

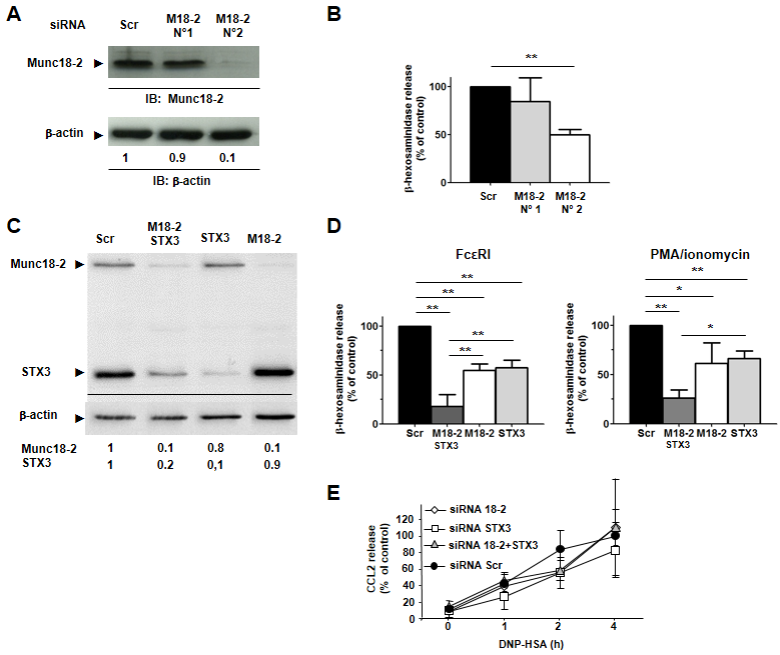

Figure 1. Additive effect of Munc18-2 and STX3 on mast cell degranulation

A) Munc18-2 expression in RBL cells treated with indicated Munc18-2-specific siRNAs. The means of relative expression levels compared to scrambled siRNA are indicated below lanes (n=6). B) Effect of Munc18-2 silencing on β-hexosaminidase release after stimulation with IgE/Ag. Results are means ± SEM of 6 experiments. ** $P < 0.01$. C) Degree of silencing of Munc18-2, STX3 or both. One representative experiment (n=3) is shown. D) Effect of silencing of Munc18-2, STX3 or both on β-hexosaminidase release after stimulation with IgE/Ag or PMA/ionomycin. Results are means ± SEM of 3 experiments. * $P < 0.05$, ** $P < 0.01$. E) Effect of silencing Munc18-2, STX3 or both on IgE/Ag-induced CCL2 chemokine secretion. Released CCL2 at 4 h in cells treated with scrambled siRNA was arbitrarily set to 100 %. Results are means ± SEM of 3 experiments.

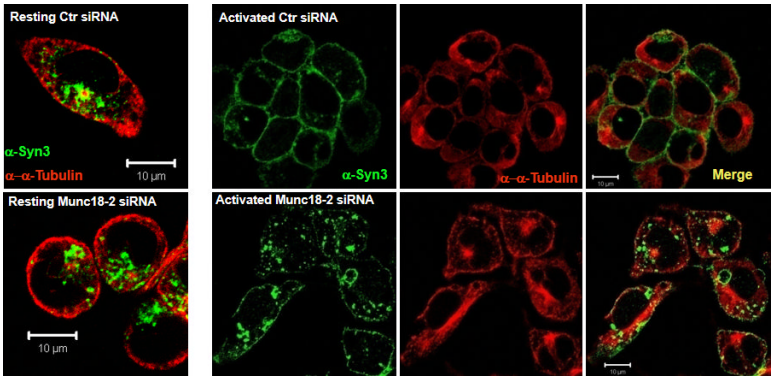

Figure 2. Munc18-2 knock-down in RBL cells inhibits SG translocation to the plasma membrane

RBL cells treated with scrambled control (upper panel) or Munc18-2 (lower panel) were grown on cover slips and stimulated with PMA/ionomycin for 20 min (right panels) or not (lefts panel). Cells were fixed, permeabilized and stained with anti-STX3 (green) and anti-αtubulin (red). Cells were visualized by confocal microscopy. Bar, 10 μm. Images shown represent single optical sections of indicated colors or the merge of two colors as indicated. Shown is one, out of five representative experiments.

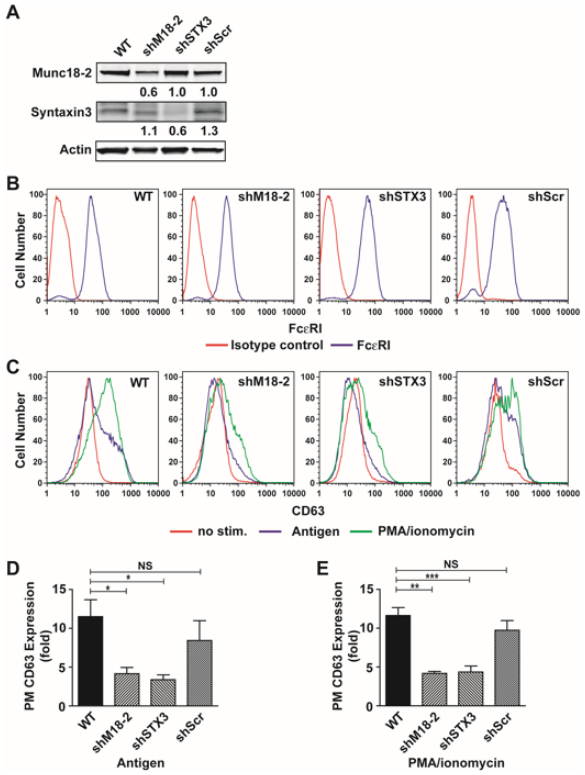

Figure 3. Impairment of granule fusion and exocytosis upon knock-down of Munc18-2 and STX3 in BMMC

(A) Expression of Munc18-2 or STX3 in WT and BMMCs treated with Munc18-2 (23B), STX3 (16B) specific shRNA or scrambled shRNA (19D). Relative expression compared to WT BMMC is indicated below lanes. Numbers are the mean of all experiments relative to WT levels. (B) Flow cytometric analysis of FcεRI expression on Munc18-2 or Synatxin3-targeted shRNA-transduced BMMCs. (C) Flow cytometric analysis of surface expression of CD63 as a surrogate degranulation marker after stimulation with IgE/Ag (blue line) or PMA/ionomycin (green line)(D, E). Quantitative analysis of CD63 expression in IgE/Ag- (D) or PMA/ionomycin-stimulated BMMCs. Data are means±SE of at least 3 independent experiments. *p<0.05, ** p<0.01, *** p<0.001.

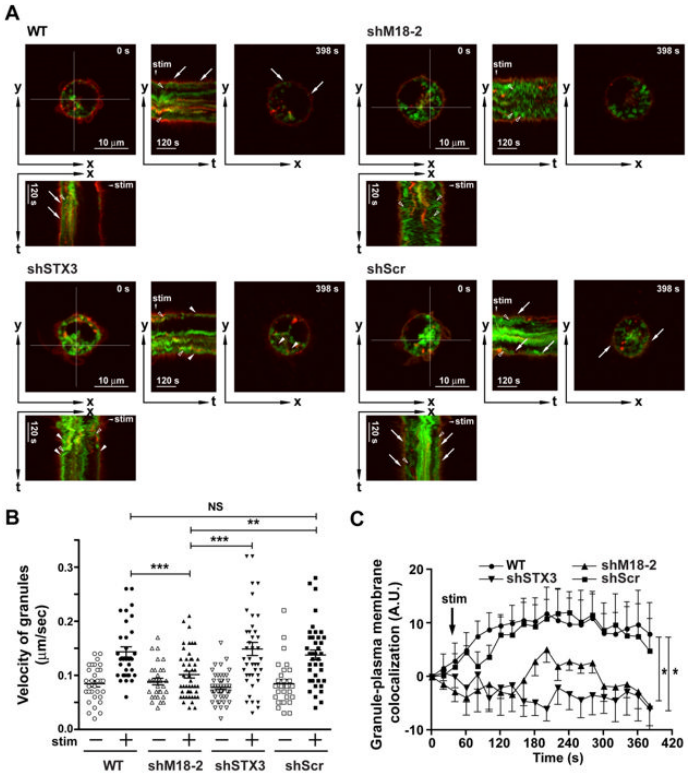

Figure 4. Silencing of Munc18-2 and STX3 in BMMC alters SG translocation and fusion, respectively

(A) Real-time imaging of secretory granule movements. CD63-GFP (green) transduced BMMCs were loaded with Alexa Fluor 555-conjugated wheat germ agglutinin (Red). The yt- or xt-images show the time-course of cross sections indicated in the xy-image (as shown in white cross section for 0 sec (0s) images). WT and control shRNA (19D) transduced BMMCs show numerous granule membrane and plasma membrane fusions (indicated by the arrows). In Munc 18-2 silenced cells (23B), few CD63-GFP positive granules moved towards the membrane and observed fusion events were rare. In Syntaxin 3 silenced cells (16B), CD63-GFP positive granules moved to the PM but fusion of granules with the PM were rare. The proximity of SG membrane with PM is indicated with an arrowhead. (B) Velocities of granules were analyzed. In Munc 18-2 silenced cells (23B), but not in Syntaxin 3 silenced cells, velocities of granules were significantly decreased. Data shown are mean +/− SE of at least 3 independent experiments. Statistical significance was **P<0.01, ***p<0.001. (C) Analysis of SG membrane and PM colocalization based on correlation coefficient analysis at the indicated time points. Data shown was normalized to the starting point (t=0). Silencing of Munc 18-2 (23B) or syntaxin 3 (16B) revealed a diminished colocalization at each time point when compared to the WT or control (19D) shRNA transduced BMMCs. Data shown are mean +/− SE of at least 4 independent experiments. Statistical significance relative to WT was *P<0.05.

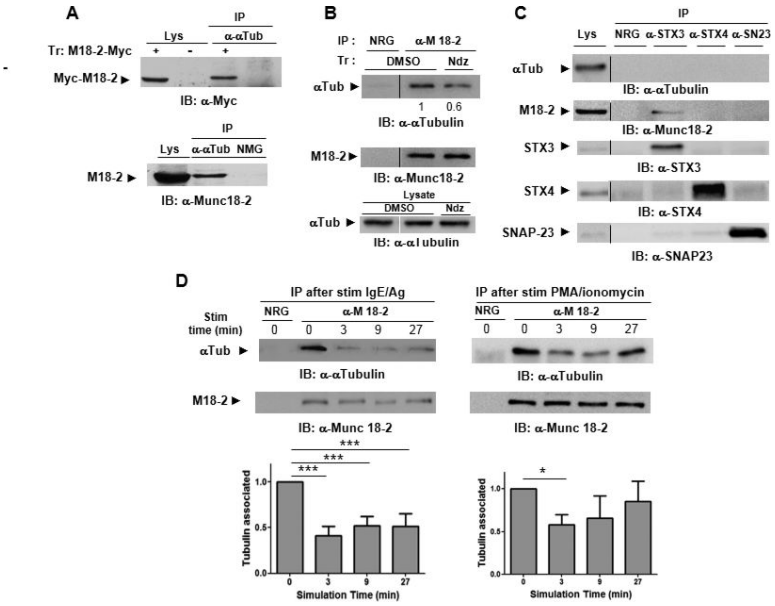

Figure 5. Munc18-2 interacts with tubulin in a stimulation dependent manner

A) Lysates (lys) from COS7 cells transfected with myc-tagged Munc18-2 (+) or empty vector (−) (upper panel) or RBL MCs were immunoprecipitated with anti-α tubulin Ab or nomal mouse IgG (NMG) as indicated before immunoblotting with anti-myc (upper panel) or anti-Munc18-2 (lower panel). B) RBL cell lysates were immunoprecipitated with anti-Munc18-2, or irrelevant normal rabbit IgG (NRG) before immunoblot analysis with indicated Abs. Relative expression levels as compared to sham-treated cells arbitrarily set to 1 are indicated below lanes. Results are representative of at least 3 independent experiments. (C) RBL cell lysates (left lane) were immunoprecipitated with irrelevant normal rabbit IgG (NRG), anti-Munc18-2, anti-STX3, anti-STX4 or anti-SNAP23 before immunoblot analysis with indicated Abs. Results are representative of at least 3 independent experiments.

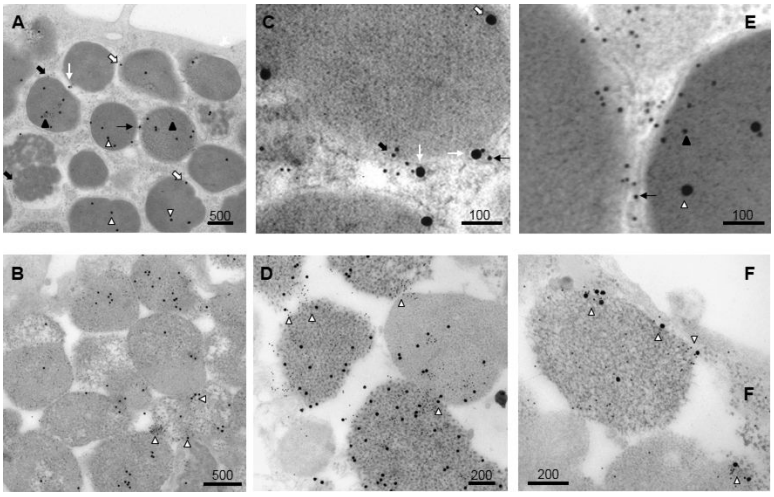

Figure 6. Ultrastructural localization of Munc18-2 and STX3 in resting and stimulated RPMC

Ultrathin sections of unstimulated RPMC (images A, C, E)) and 48/80 stimulated RPMC (images B, D, F) were double-immunogold labelled with anti-Munc18-2 (10 nm gold particles) and anti-STX3 (20 nm gold particles). Cells were visualized by electron microscopy. Bars are in nm as indicated. In unstimulated cells Munc18-2 and STX3 are present either on the granular surface or within granules as indicated by arrows as explained in the text. Munc18-2 are often accumulating in tangles at filamentous connections between SG that sometimes also contain STX3 (C, E). In stimulated cells, such tangles can be seen to concentrate at fusion sites either between SG (D) or at the PM (F), where they are enriched in both Munc18-2 and STX3 GPs as shown by the arrows.

Table 1

Subcellular distribution of Munc18-2 and Syntaxin3 in RPMC and effect of nocodazol and taxol treatment.

	Munc18-2 GP			Syntaxin3 GP		
Treatment	**SG surface**	**SG matrix**	**Filamentous Connections**	**SG surface**	**SG matrix**	**Filamentous Connections**
No treatment (25)	13.8 ± 0.9[a]	66.4 ± 5.0	19.9 ± 5.0	22.5 ± 2.7	68.1 ± 3.0	9.4 ± 2.1
Nocodazole (17)	**26.9 ± 3.9**[b] p < 0.001	67.9 ± 3.7	*3.3 ± 1.6*	**38.8 ± 6.4** p < 0.02	54.9 ± 5.1	4.4 ± 2.2
Taxol (16)	**29.4 ± 2.5** p = 0.001	66.0 ± 4.5	*4.5 ± 1.4*	31.4 ± 5.1	67.8 ± 5.1	**0.8 ± 0.6** p < 0.02

[a] Values are the mean (± SEM) of the % of Gold Particles (GP) in each subcellular compartment taking the total number of GPs in each picture as 100 %. The numbers of pictures scored is shown in parenthesis. Total GPs scored were at least 200 and 1500 for Syntaxin3 and Munc18-2, respectively

[b] Numbers in bold indicate statistical significant differences as compared to untreated cells. Statistical analysis was carried out using GraphPAD Prism5 program. P was calculated using Student's t test for unpaired data, two tailed.